Title

Differential effects of targeting Notch receptors in a mouse model of liver cancer

Authors

Huntzicker, Erik G
Hötzel, Kathy
Choy, Lisa
et al.

Peer reviewed

Differential effects of targeting Notch receptors in a mouse model of liver cancer

Erik G. Huntzicker[1], **Kathy Hötzel**[4], **Lisa Choy**[3], **Li Che**[2], **Jed Ross**[5], **Gregoire Pau**[6], **Neeraj Sharma**[4], **Christian W. Siebel**[3], **Xin Chen**[2], and **Dorothy M. French**[1]

[1]Pathology Department Biomarker Group, Gilead Sciences

[2]Department of Bioengineering and Therapeutic Sciences, University of California, San Francisco

[3]Department of Discovery Onoclogy, Genentech

[4]Department of Research Pathology, Genentech

[5]Department of Biomedical Engineering, Genentech

[6]Department of Bioinformatics and Computational Biology, Genentech

Abstract

Primary liver cancer encompasses both hepatocellular carcinoma (HCC) and cholangiocarcinoma (CC). The Notch signaling pathway, known to be important for the proper development of liver architecture, is also a potential driver of primary liver cancer. However, with four known Notch receptors and several Notch ligands, it is not clear which Notch pathway members play the predominant role in liver cancer. To address this question we utilized antibodies to specifically target Notch1, Notch2, Notch3 or Jag1 in a mouse model of primary liver cancer driven by AKT and NRas. We show that inhibition of Notch2 reduces tumor burden by eliminating highly malignant hepatocellular carcinoma- and cholangiocarcinoma-like tumors. Inhibition of the Notch ligand Jag 1 had a similar effect, consistent with Jag1 acting in cooperation with Notch2. This effect was specific to Notch2, as Notch3 inhibition did not decrease tumor burden. Unexpectedly, Notch1 inhibition altered the relative proportion of tumor types, reducing HCC-like tumors but dramatically increasing CC-like tumors. Finally, we show that Notch2 and Jag1 are expressed in, and Notch2 signaling is activated in, a subset of human HCC samples. Conclusions: These findings underscore the distinct roles of different Notch receptors in the liver and suggest that inhibition of Notch2 signaling represents a novel therapeutic option in the treatment of liver cancer.

Keywords

hepatocellular carcinoma; cholangiocarcinoma; Ras; AKT

Introduction

Liver cancer comprises both hepatocellular carcinoma (HCC) and intrahepatic cholangiocarcinoma (CC) and is the fifth most common form of cancer in the world. Each year, approximately 750,000 cases are diagnosed (1) while 700,000 people die from the disease, making it the third most common cause of cancer death world-wide (1). While some progress has been made in detecting and treating localized disease, the five year survival rate for late stage liver cancer is still well below 10%(2).

While increasing evidence points to a role for Notch signaling in liver cancer, this role is controversial and not yet well understood. For example, some studies show that expression of the constitutively active form of Notch1 has an inhibitory effect on HCC tumor cells(3), and blocking Notch with γ-secretase inhibitors (GSI) in mice promotes HCC development, suggesting that Notch might function as a tumor suppressor (3, 4). However other studies have shown that Notch signaling can drive HCC tumor growth and that inhibition of the pathway has an anti-tumor effect (5, 6). Recently, several studies have suggested that Notch signaling functions as a driver of liver tumors(6–9).

It is important to note that in most of the studies constitutively activated Notch receptors were used. These activated Notch receptors may stimulate unnaturally high levels of signaling not observed when Notch is regulated endogenously via its ligands. In addition, γ-secretase is not specific to Notch signaling and is involved in the cleavage and activation of other substrates, including EpCAM (10), which is highly expressed in a subset of human HCC (11). Moreover, Notch's function during tumorigenesis is likely cell-type specific and oncogene dependent, and it is possible that different Notch receptors could have distinct functional roles in carcinogenesis. It is therefore important to study the role of Notch signaling when Notch receptors are physiologically activated via their ligands. In this manuscript we report the activation of the Notch pathway in liver tumors induced by activated AKT and NRas proto-oncogenes. Importantly, using specific antagonistic antibodies, we demonstrate that inhibition of Notch1 or Notch2 results in distinct phenotypes. These observations provide evidence, for the first time, that different Notch receptors have drastically different functions during liver cancer development. Our studies also support the use of anti-Notch2 based therapy in treating liver cancer.

Experimental Procedures

Hydrodynamic tail vein injection

FVB-N mice (Charles River, Hollister, CA) were subjected to hydrodynamic tail vein injection of Ras, AKT, and Sleeping Beauty transposase encoding plasmids as previously described(12). On the day of the hydrodynamic tail vein injection, treatment with antagonistic antibodies to Notch1 (13), Notch2 (13), Notch3 (Siebel C, unpublished data), or Jag1 (Siebel C, unpublished data) was begun at doses indicated in text. For the intervention experiment, dosing was begun 2 weeks or 3 weeks after HTV injection. An anti-Ragweed antibody, designated "Isotype Control", was used as a negative control and dosed as indicated in text. All animal experiments were conducted in compliance with National

Institute of Health Guide for the Care and Use of Laboratory Animals and were approved by the Genentech Institutional Animal Care and Use Committee.

Immunofluorescence

Immunofluorescence was performed on 7μm frozen liver sections using labeled antibodies to EpCAM (BioLegend, San Diego, CA), or with unlabeled primary antibodies to AFP (R&D Systems), CD31 (BD Biosciences, San Jose CA) Notch1 (Cell Signaling Technology, Danvers, MA), or Notch2 (Cell Signaling Technology, Danvers, MA) followed by incubation with fluorescently labeled secondary antibodies (Alexafluor 488, 568, 594 647, Life Technologies, Grand Island, NY, or Cy3, Jackson ImmunoResearch, West Grove, PA). A list of antibodies is provided in the Supplementary Table 1.

qRT-PCR

Quantitative real-time PCR (QRTPCR) was performed using the TaqMan One-Step RT-PCR Kit for one step reactions using the 7900 HT RT-PCR system (Life Technologies, Grand Island, NY) with TaqMan probes (Life Technologies, Grand Island, NY). A list of primers and probes is provided in the Supplementary Table 2.

Detailed description of Materials and Methods can be found in the Supplement.

Results

The AKT/Ras model recapitulates the spectrum of human liver cancer

Coordinated activation of Ras/MAPK and AKT/mTOR cascades is frequently observed in human liver cancers. We therefore utilized a murine liver tumor model generated by transfecting activated forms of Akt (myr-Akt) and Ras (NRasV12) oncogenes together with sleeping beauty transposase via hydrodynamic tail vein injection (HTV), which allows targeting of genes to hepatocytes for long-term expression with efficiency of 2 to 10%(12). Ho et al. previously observed that HTV injection of AKT alone leads to hepatic steatosis and eventually tumor formation at 6 months post injection. HTV of Ras does not lead to any abnormal liver phenotype. In contrast, co-HTV injection of Ras and AKT (AKT/Ras) significantly accelerated AKT-induced liver tumor formation: pre-neoplastic lesions could be observed as early as one week post-injection and they expanded to occupy over 50% of the liver at 3 weeks post-injection. At this stage, highly malignant liver tumors start to emerge. The tumors rapidly expand, occupying over 80% of the liver parenchyma and lead to lethality by 5 to 6 weeks post-injection (12). At this stage, tumors were confirmed to express the HA-tagged AKT construct as shown by HA immunofluorescence (Supplementary Figure 1F). The tumors in these mice comprised a spectrum of morphologic types from HCC-like tumors to CC-like tumors and tumors with mixed morphology (Figure 1A–C)(12). Histologically, liver from isotype control treated AKT/Ras mice was distorted and replaced by large, coalescing, expansile nodules composed of densely packed neoplastic hepatocytes similar to tumors described previously for the AKT/Ras model(12). Neoplastic cells were arranged either in dense sheets, trabeculae or in tubules with occasional areas of necrosis (Figure 1A–C). Neoplastic cells were either small and basophilic with large, pleomorphic, hyperchromic nuclei and scant cytoplasm or large and polygonal with

abundant, amphophilic, occasionally vacuolated cytoplasm and one to several ovoid, vesicular nuclei. Interestingly, nodules were often composed predominantly of one phenotype, small and basophilic or large and polygonal (Figure 1A–B), or a mixture of both phenotypes of neoplastic cells, suggesting distinct cell origins (cholangiocyte versus hepatocyte, Figure 1C). Hepatic parenchyma adjacent to and compressed by the neoplastic nodules was composed of altered hepatocytes, often markedly enlarged with vacuolated, clear to foamy cytoplasm. Although histologic evaluation of the livers from AKT/Ras HTV mice in this study was consistent with previously published descriptions(12), we also sought to characterize the tumor nodules by immunofluorescence to quantify the tumor subtypes. The tumors that developed in this model varied according to the expression of the HCC-specific marker AFP (Figure 1D) (14) and the CC-associated marker EpCAM (Figure 1E) (15). AFP marked an average of 12.8% of cells in tumor-bearing livers (Figure 1G). EpCAM was less prevalent, staining about 5% of all liver cells (Figure 1G). Interestingly, up to 9% of cells expressed both markers, identifying them as possible combined HCC-CC (cHCC-CC), a tumor type with particularly aggressive clinical features(16).

Notch2 signaling is active in tumors of the AKT/Ras model

Cholangiocarcinomas and cHCC-CC tumors share gene expression patterns with liver progenitor cells(16). Consistent with the observation that Notch signaling is active in liver progenitor cells(17) we found high levels of Notch2 activation as determined by immunofluorescent detection of nuclear Notch2: average of 40% in AFP+/EpCAM+ tumors and average of 20% in EpCAM+ tumors (Figure 1H, I). Active Notch2 is present in the AFP + and AFP−/EpCAM− cell populations (Fig. 1I) albeit to a lesser extent. Notch1 was also expressed in the tumor-bearing livers, but was largely confined to CD31-positive endothelial cells (Figure 2A) similar to normal, non-tumor bearing mouse liver (Supplementary Figure 1A). Robust expression of Notch1 on tumor epithelium was seen in some instances (Figure 2B, left panel), but staining with an antibody to the γ-secretase-cleaved, active form of Notch1 (Figure 2B, right panel) revealed that Notch1 signaling was not active in these tumors except in endothelial cells and Kupffer cells. By Western blot, Notch2 and Jag1 are clearly upregulated in the AKT/Ras liver relative to wild-type liver whereas Notch1 protein was unchanged (Supplementary Figure 1 D). QRT-PCR confirmed the up-regulation of *notch2* and unchanged *notch1* mRNA (Supplementary Figure 1E). Immunohistochemical detection of Notch2 in wild-type mouse revealed distinctly membranous staining on sinusoids and bile duct epithelium (Suplementary Figure 1B), whereas Notch1 was expressed on sinusoidal, Kupffer cell and endothelial membranes (Supplementary Figure 1A). Similar staining patterns were seen in normal human liver for both Notch1 and Notch2 (Supplementary Figure 1C). Hes1, a downstream target of Notch signaling, was shown by immunohistochemistry to be strongly expressed by CC-like tumors and was also expressed, although slightly weaker, in HCC-like nodules (Supplementary Figure 2).

Anti-Notch2 or anti-Jag1 antibody treatments reduce tumor burden in AKT/Ras model

These observations led us to propose that Notch2 signaling was important for driving the development or growth of the AKT/Ras liver tumors. We therefore treated AKT/Ras HTV animals with anti-Notch2 antagonistic antibody (13), anti-Jag1 antagonistic antibody, or isotype control beginning the day of the HTV injection. Mice treated with the control

antibody developed a heavy tumor burden (Figure 3A) five weeks following HTV injection, with their livers increasing on average to 31% of body weight, up from 5.8% of body weight (Figure 3B) in normal liver. Mice treated with anti-Notch2 or anti-Jag1 antibody developed a smaller tumor burden with their livers growing to 19.3% and 15.8% of body weight, respectively (Figure 3B).

In keeping with the effect of Notch2 and Jag1 inhibition on tumor formation, we found that Notch2 signaling – as determined by immunofluorescent detection of nuclear Notch2 protein – was reduced throughout the tumor-bearing livers with either anti-Notch2 or anti-Jag1 treatment (Figure 3C). This was due to a direct effect on activation of the Notch2 protein, as overall levels of Notch2 expression, determined by QRT-PCR, did not change (Figure 3D). Consistent with antibody treatment blocking Notch2 activation, we found a reduction in immunostaining for Hes1 (Figure 3E, Supplementary Figure 3). Confirming that Notch signaling was blocked, quantitative RT-PCR analysis revealed that the Notch pathway target gene HeyL was also strongly decreased with antibody treatment (Figure 3F). In each case, anti-Jag1 treatment had the same effect as anti-Notch2 treatment, supporting the conclusion that Jag1 acted as a ligand for Notch2 to promote tumor formation. Histologically, in striking contrast to control-treated animals, livers from anti-Notch2 or anti-Jag1 animals were composed mainly of altered hepatocyte foci (Figure 4E). The altered hepatocytes had abundant clear or vacuolated cytoplasm that resulted in marked enlargement of the hepatocytes; however, cellular and nuclear atypia, invasive growth, and replacement of hepatic architecture were not present (Figure 4E). Additionally, we observed decreased numbers of Ki67 positive cells in the Notch2 antibody-treated liver tissues (Supplementary figure 4).

Notch2 inhibition prevents tumor formation and reduces existing tumor burden

Treatment with anti-Notch2 or anti-Jag1 antibodies beginning the day of HTV injection almost completely prevented tumorigenesis. It was unknown whether anti-Notch2 or anti-Jag1 treatment could impact the growth of tumor lesions after they arise. To distinguish between prevention and intervention, treatment was begun at two weeks after HTV AKT/Ras injection, a time when the liver significantly increases in size(12) and at three weeks when tumors have already become established as determined by MRI in our study (Supplementary figure 5A). When antibody treatment was begun two weeks after HTV injection, Notch2 or Jag1 inhibition resulted in diminished tumor burden as reflected in smaller liver size (Supplementary Figure 5B). Similar results were obtained when antibody treatment was begun three weeks after HTV injection (Supplementary Figure 5C). Following treatment with anti-Notch2 or anti-Jag1 in the 3-week-post HTV treatment groups, the few tumors that remained had prominent central necrosis (Supplementary Figure 5 E, arrows). Therefore, it is likely that anti-Notch2 or anti-Jag1 not only prevented tumor formation but also affected established tumors to decrease tumor burden in the intervention study.

Inhibition of Notch1 reduces HCC-like tumors but increases CC-like tumors

We next sought to evaluate the role of other Notch receptors in this model including Notch1 and Notch3. Treatment with an anti-Notch1 antibody had a similar effect on liver weight to

Notch2 inhibition, while treatment with a Notch3 antibody had no significant effect (Figure 4A). Interestingly, histopathological examination revealed that while Notch2 and Jag1 inhibition led to an overall lower tumor burden (Figure 4B), inhibition of Notch1 only led to a lower number of large HCC-like tumors (Figure 4C–E). Histological evaluation to assess the overall percentage of liver tissue occupied by tumors and to enumerate morphologic subtypes of liver tumor demonstrated that anti-Notch2 or anti-Jag1 reduced overall tumor burden from a mean of 80% in the isotype control-treated mice to a mean of 11% and 12% for anti-Notch2 and anti-Jag1 treated mice, respectively (Figure 4B). Anti-Notch2 or anti-Jag1 treatment reduced all morphologic subtypes of liver tumor: for HCC-like tumors the mean was 29 in isotype treated, mean=8 in anti-Notch2 treated, and mean=12 in anti-Jag1 treated groups. For CC-like tumors the mean was 9 in the isotype treated, mean=0 in the anti-Notch2 treated, and mean=1 in the anti-Jag1 treated group. For mixed tumors the mean was 6 in isotype treated, mean=0 in anti-Notch2 treated and mean=1 in anti-Jag1 treated mice (Figure 4C–E). Anti-Notch1 reduced overall tumor burden (% area) by 43% (Figure 4B); however, enumeration of morphologic subtypes of tumor nodules demonstrated that anti-Notch1 reduced HCC-like tumors by 86% (from mean=29 in istotype treated to mean=4 in anti-Notch1 treated mice) but increased CC-like nodules by 78% (mean=9 for isotype and mean=42 for anti-Notch1 treated mice) relative to tumors from control treated AKT/Ras mice (Figure 4C–E). Immunofluorescent quantification of tumor subtypes confirmed the histologic enumeration. For the EpCAM-positive tumors, quantification showed this population was virtually eliminated with anti-Notch2 or anti-Jag1 treatment, while anti-Notch3 had no effect (Figure 5A–B). In contrast, inhibition of Notch1 increased the relative area of EpCAM-positive tumors in the liver by almost two fold (Figure 5A–B), consistent with the observed increase in CC-like tumors determined by morphological examination (Figure 4C–E). The lower HCC-like tumor burden seen with anti-Notch1 treatment was reflected in reduced AFP positive tumor area (Supplemental Figure 6). Tumor proliferation, as revealed by Ki67 staining, was not decreased by Notch1 inhibition as it was for Notch2 (Supplementary Figure 4A).

Anti-Notch2 treatment results in decreased activated Notch2 protein and changed transcriptional signature—We subsequently assessed activation of Notch2 in the tumor bearing livers with a novel antibody (Supplementary Figure 7) specific to the cleaved, active form of Notch2 (Notch2 ICD). Treatment with anti-Notch2 or anti-Jag1 antibody led to a disappearance of activated Notch2 as determined by Western blot (Figure 6A–B). In contrast, Notch3 inhibition did not affect Notch2 activation(Figure 6B). Intriguingly, anti-Notch1 treatment led to an increase in Notch2 ICD levels (Figure 6B). The same observations were borne out by immunofluorescence, where Notch2 activation was determined by nuclear localization of Notch2 signal (Figure 6C).

Although Notch2 activation was clearly implicated in tumorigenesis we also sought to understand molecular changes leading to reduced tumor burden. RNA-Seq analysis revealed significantly decreased expression of forkhead box M1 (FOXM1) and FOXM1 targets(12), Aurora B and Plk1, in anti-Notch2 or anti-Jag1 treated groups relative to the isotype treated group (Supplementary Figure 8A). These genes were not altered in the anti-Notch1 or anti-Notch3 treated groups relative to the isotype group. In addition to FOXM1 we discovered

alterations in differentiation markers. There was significant elevation of transcripts associated with hepatocellular differentiation including Hnf4alpha, Glutamine Sythetase and FAH (Supplementary Figure 8B).

Notch2 and Jag1 are expressed in a subset of human HCCs

Next, we analyzed human tumor specimens for Notch2 and Jag1 expression by IHC. We found prominent expression of Notch2 in 28 of 76 (37%) HCC samples. In 15 of these 28 cases (54%) Notch2 showed varying degrees of nuclear localization indicating Notch2 pathway activation. Jag1 was expressed in 34 of 59 (57%) human HCCs examined. Of the 56 cases evaluated for both Notch2 and Jag1, 22 of the cases expressed both proteins (39%). Of those 22 cases with overlapping expression, 15 (68%) showed some degree of Notch2 nuclear localization indicating active Notch2 signaling. To further determine association with EpCAM, immunohistochemistry for EpCAM expression was performed on 25 of the cases with Notch2 expression. Interestingly, 9/14 (64%) of the Notch2 activated cases showed prominent EpCAM immunoreactivity. A representative HCC case with membranous Notch1 (Figure 7A) and overlapping nuclear Notch2, Jag1, Hes1 and EpCAM staining is shown (Figure 7B–E). Only 2/11 cases that did not have nuclear Notch2 were EpCAM positive whereas the remaining 9 cases were EpCAM negative (Figure 7F). These data are suggestive of a progenitor-like or CC-like phenotype in the Notch2 activated subset of HCCs. Lastly, to determine whether Notch1 was expressed, we evaluated a total of 52 human HCC cases for Notch1 expression: 28 cases that had prominent Notch2 expression and an additional 24 cases that did not have Notch2 expression. IHC using the total Notch1 antibody showed prominent membranous immunoreactivity in 14/28 Notch2-positive cases and 8/24 of the Notch2-negative cases (total of 42%, 22/52 cases, positive for membranous Notch1). None of the cases had nuclear Notch1 in neoplastic cells when evaluated with the Notch1 ICD-specific antibody but did show nuclear staining in occasional endothelial cells and Kupffer cells (Supplementary Figure 9).

Discussion

In this study we have shown that anti-Notch2 treatment blocked the development of a broad range of tumors in a mouse model of primary liver cancer. Inhibition of Jag1 had the same effect on blocking tumor formation as inhibition of Notch2, suggesting that Jag1 acted as a ligand for Notch2 in this setting (Figure 3). We have also demonstrated that both antibodies are effective at reducing tumor burden in an intervention setting, where antibody treatment is started only after tumor formation has begun.

In contrast, treatment with anti-Notch1 caused a striking increase in the number and extent of EpCAM-positive cholangiocarcinoma-like tumors (Figures 4 and 5). This is significant in light of contradictory studies regarding the effect of Notch pathway inhibition in liver cancer(4, 5). However, previous studies accomplished Notch pathway blockade through utilizing gamma-secretase inhibitors (GSIs). GSIs are broad inhibitors of Notch activation, affecting a processing pathway common to all four Notch receptors. Moreover, since gamma-secretase is involved in the cleavage of other substrates(18) and the regulation of other signaling pathways(10), GSI administration will potentially have pleiotropic and

contradictory effects on cancer cells. Our results reveal strikingly divergent roles for the different Notch receptors in our mouse model of liver cancer using highly specific antibodies that lead to selective inhibition of Notch receptors or ligands.

Evaluation of potential molecular mechanisms underlying efficacy of Notch2/Jag1 inhibition in the AKT/Ras model revealed decreased FOXM1, and FOXM1 target genes Aurora B and Plk1, expression. FOXM1 is a transcription factor that was previously implicated in the molecular pathogenesis of the Akt/Ras liver tumor model. (12) Therefore, direct or indirect inhibition of FOXM1 and its target genes by anti-Notch2 or anti-Jag1 could be part of the mechanism of tumor inhibition in our studies. FOXM1 has also been described as a Notch target in prostate cancer where Notch1 was shown to be highly expressed and Notch1 siRNA resulted in reduction of FOXM1 concomitant with reduced Notch1 ICD protein(19).

While multiple studies have attempted to determine the expression pattern of Notch1 in human HCC samples, the results have thus far been inconsistent and controversial, from membrane or cytoplasm staining in 50% of HCC samples (20)with no nuclear localization of Notch1 in HCCs to nuclear staining of Notch1 in 49% of all HCC analyzed(21). Interestingly, when we evaluated 62 HCC cases using an antibody specific for total Notch1 we found that 35% were positive for membranous Notch1 but, using an antibody specific for cleaved Notch1 (Figure 2B and Supplementary Figure 10), none of the HCC cases were positive for nuclear Notch1 in the neoplastic cells although endothelial cells, Kupffer cells and occasional infiltrating cells were positive for cleaved Notch1 (Figure 2B). This highlights the variability of Notch IHC reagents and emphasizes the need to carefully validate antibody specificity prior to use.

The fact that activated Notch1 expression is located on endothelial cells suggests that the effects may be mediated via paracrine mechanisms. For example, it is possible that inhibiting Notch1 in endothelial cells may lead to the increased expression of Notch ligands in these cells, and the ligands can further activate Notch2 in the adjacent hepatocytes. Of note, Notch1 inhibition in the AKT/Ras model did not result in aberrant endothelial proliferation (Supplementary Figure 11) as described in other studies(22) (6). And it was interesting that, although the liver weight decreased in the anti-Notch1 treated animals, proliferation as determined by Ki67 was not different from isotype control-treated mice (Supplementary Figure 4). It is unclear, though, why the liver weight goes down in the anti-Notch1 treated group although we speculate that it is due to reduced HCC-like tumor burden as evidenced by histological evaluation and EpCAM IF (Figure 5) but did not affect lipid accumulation or mTOR pathway (Supplementary Figure 12).

Our current studies suggest the therapeutic potential of Anti-Notch2 or Anti-Jag1 for liver cancer based on efficacy in the AKT/Ras model. It should be noted, however, that some toxicity was observed, particularly at higher doses of antibody. This manifested largely in the form of weight loss. Nevertheless, Notch2 inhibition did confer a slight survival advantage over the isotype control-treated group (Supplementary Figure 13). Although the analysis did not meet criteria for statistical significance (HR 0.3342, p=0.0776) the mice did not die with a heavy tumor burden. It would be of great interest to determine Notch pathway activation status in other murine liver cancer models such as liver tumors induced by DENA

carcinogen or other oncogenes including c-Myc or c-Met/β-catenin. Future studies with anti-Notch specific antibodies in these mouse liver tumor models will provide additional insight into the usefulness of anti-Notch based therapeutics in treating this deadly malignancy and may offer a novel therapeutic avenue in this difficult-to-treat disease.

Supplementary Material

Refer to Web version on PubMed Central for supplementary material.

Acknowledgments

Abbreviations

AKT	v-akt murine thymoma viral oncogene homolog
NRas	Neuroblastoma RAS viral oncogene homolog
Jag1	Jagged 1
HCC	Hepatocellular carcinoma
CC	cholangiocarcinoma
EpCAM	Epithelial Cell adhesion molecule
AFP	alpha fetoprotein
Hes1	Hairy and enhancer of split 1
HeyL	Hairy/enhancer of split related with YRPW motif-like
Notch2 ICD	Notch2 intracellular domain

References

1. Ferlay J, Shin HR, Bray F, Forman D, Mathers C, Parkin DM. Estimates of worldwide burden of cancer in 2008: GLOBOCAN 2008. Int J Cancer. 2010; 127:2893–2917. [PubMed: 21351269]

2. American-Cancer-Society. Cancer Facts & Figures 2012. Atlanta: American Cancer Society; 2012.

3. Qi R, An H, Yu Y, Zhang M, Liu S, Xu H, Guo Z, et al. Notch1 Signaling Inhibits Growth of Human Hepatocellular Carcinoma through Induction of Cell Cycle Arrest and Apoptosis. Cancer Research. 2003; 63:8323–8329. [PubMed: 14678992]

4. Viatour P, Ehmer U, Saddic LA, Dorrell C, Andersen JB, Lin C, Zmoos AF, et al. Notch signaling inhibits hepatocellular carcinoma following inactivation of the RB pathway. J Exp Med. 2011; 208:1963–1976. [PubMed: 21875955]

5. Villanueva A, Alsinet C, Yanger K, Hoshida Y, Zong Y, Toffanin S, Rodriguez–Carunchio L, et al. Notch Signaling Is Activated in Human Hepatocellular Carcinoma and Induces Tumor Formation in Mice. Gastroenterology. 2012; 143:1660–1669. e1667. [PubMed: 22974708]

6. Dill MT, Tornillo L, Fritzius T, Terracciano L, Semela D, Bettler B, Heim MH, et al. Constitutive Notch2 signaling induces hepatic tumors in mice. Hepatology. 2013:n/a–n/a.

7. Fan B, Malato Y, Calvisi DF, Naqvi S, Razumilava N, Ribback S, Gores GJ, et al. Cholangiocarcinomas can originate from hepatocytes in mice. J Clin Invest. 2012; 122:2911–2915. [PubMed: 22797301]

8. Sekiya S, Suzuki A. Intrahepatic cholangiocarcinoma can arise from Notch-mediated conversion of hepatocytes. J Clin Invest. 2012; 122:3914–3918. [PubMed: 23023701]

9. Zender S, Nickeleit I, Wuestefeld T, Sorensen I, Dauch D, Bozko P, El-Khatib M, et al. A critical role for notch signaling in the formation of cholangiocellular carcinomas. Cancer Cell. 2013; 23:784–795. [PubMed: 23727022]

10. Denzel S, Maetzel D, Mack B, Eggert C, Barr G, Gires O. Initial activation of EpCAM cleavage via cell-to-cell contact. BMC Cancer. 2009; 9:402. [PubMed: 19925656]

11. Yamashita T, Forgues M, Wang W, Kim JW, Ye Q, Jia H, Budhu A, et al. EpCAM and alpha-fetoprotein expression defines novel prognostic subtypes of hepatocellular carcinoma. Cancer Res. 2008; 68:1451–1461. [PubMed: 18316609]

12. Ho C, Wang C, Mattu S, Destefanis G, Ladu S, Delogu S, Armbruster J, et al. AKT (v-akt murine thymoma viral oncogene homolog 1) and N-Ras (neuroblastoma ras viral oncogene homolog) coactivation in the mouse liver promotes rapid carcinogenesis by way of mTOR (mammalian target of rapamycin complex 1), FOXM1 (forkhead box M1)/SKP2, and c-Myc pathways. Hepatology. 2012; 55:833–845. [PubMed: 21993994]

13. Wu Y, Cain-Hom C, Choy L, Hagenbeek TJ, de Leon GP, Chen Y, Finkle D, et al. Therapeutic antibody targeting of individual Notch receptors. Nature. 2010; 464:1052–1057. [PubMed: 20393564]

14. Shiota G, Miura N. Biomarkers for hepatocellular carcinoma. Clinical Journal of Gastroenterology. 2012; 5:177–182.

15. de Boer CJ, van Krieken JHJM, Janssen-van Rhijn CM, Litvinov SV. Expression of Ep-CAM in normal, regenerating, metaplastic, and neoplastic liver. The Journal of Pathology. 1999; 188:201–206. [PubMed: 10398165]

16. Coulouarn C, Cavard C, Rubbia-Brandt L, Audebourg A, Dumont F, Jacques S, Just PA, et al. Combined hepatocellular-cholangiocarcinomas exhibit progenitor features and activation of Wnt and TGFbeta signaling pathways. Carcinogenesis. 2012; 33:1791–1796. [PubMed: 22696594]

17. Boulter L, Govaere O, Bird TG, Radulescu S, Ramachandran P, Pellicoro A, Ridgway RA, et al. Macrophage-derived Wnt opposes Notch signaling to specify hepatic progenitor cell fate in chronic liver disease. Nat Med. 2012 advance online publication.

18. Hemming ML, Elias JE, Gygi SP, Selkoe DJ. Proteomic Profiling of γ-Secretase Substrates and Mapping of Substrate Requirements. PLoS Biol. 2008; 6:e257. [PubMed: 18942891]

19. Wang Z, Li Y, Ahmad A, Banerjee S, Azmi AS, Kong D, Wojewoda C, et al. Down-regulation of Notch-1 is associated with Akt and FoxM1 in inducing cell growth inhibition and apoptosis in prostate cancer cells. Journal of Cellular Biochemistry. 2011; 112:78–88. [PubMed: 20658545]

20. Ahn S, Hyeon J, Park CK. Notch1 and Notch4 are markers for poor prognosis of hepatocellular carcinoma. Hepatobiliary Pancreat Dis Int. 2013; 12:286–294. [PubMed: 23742774]

21. Tschaharganeh DF, Chen X, Latzko P, Malz M, Gaida MM, Felix K, Ladu S, et al. Yes-associated protein up-regulates Jagged-1 and activates the Notch pathway in human hepatocellular carcinoma. Gastroenterology. 2013; 144:1530–1542. e1512. [PubMed: 23419361]

22. Croquelois A, Blindenbacher A, Terracciano L, Wang X, Langer I, Radtke F, Heim MH. Inducible inactivation of Notch1 causes nodular regenerative hyperplasia in mice. Hepatology. 2005; 41:487–496. [PubMed: 15723439]
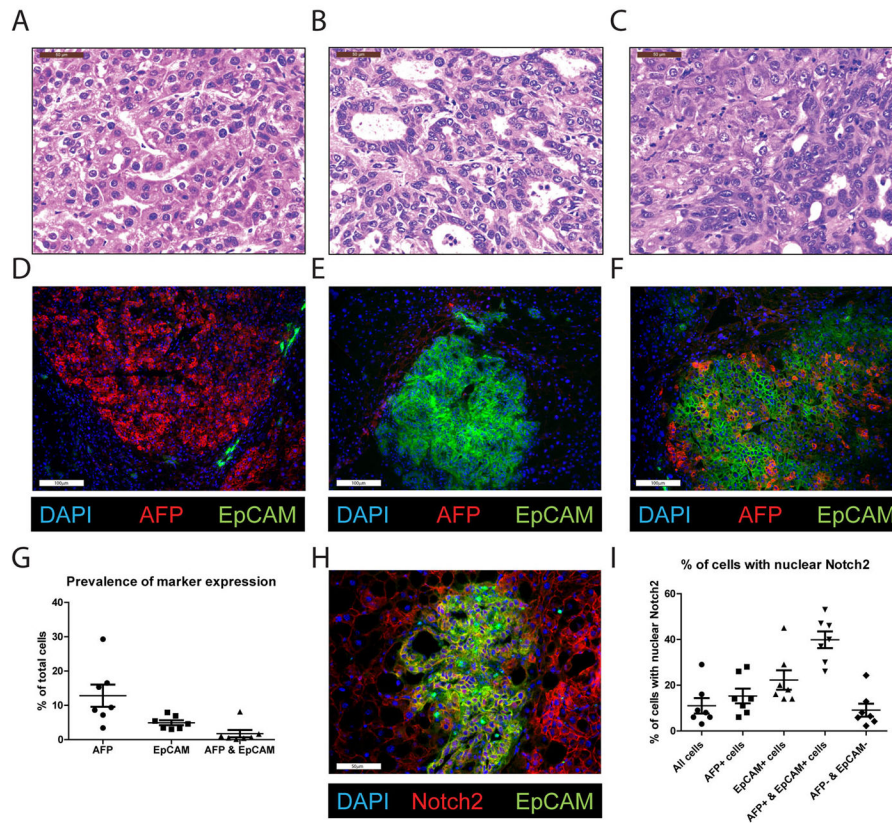
Figure 1.
Characterization of tumors in the AKT/Ras HTV model. (A–C) In the AKT/Ras HTV tumor model numerous tumors arose in a single liver and reflected the range of morphologies seen in human liver cancer. (Scale bar = 50μm). These included (A) hepatocellular carcinoma-like tumors, (B) cholangiocarcinoma-like tumors, and (C) tumors with mixed hepatocellular carcinoma-like and cholangiocarcinoma-like features. (D–F) Different tumor nodule types expressed markers commonly found in the corresponding human liver tumor types (Scale Bar = 100μm). (D) AFP was expressed primarily in livers with HCC morphology, while (E) EpCAM was found primarily in cholangiocarcinoma-like tumors. (F) Some HCC-like tumors expressed both AFP and EpCAM. (G) Relative abundance of tumor markers, AFP and EpCAM, by quantitative morphometry on whole slide scans of tumor bearing liver sections. Values represent the percentage of all nucleated cells positive for a marker or combination of markers in the whole liver cross-section. (H) Some cells showed active Notch signaling as revealed by immunofluorescent staining of Notch2 in the nucleus (Scale bar = 50μm). (I) Activation of Notch2 was most prominent in cells double-positive for AFP and EpCAM and for cells expressing EpCAM alone, with less prominent staining in other tumor cell types. Values represent the percentage of Notch2 positive cells in the population of all nucleated cells positive for a marker or combination of markers.
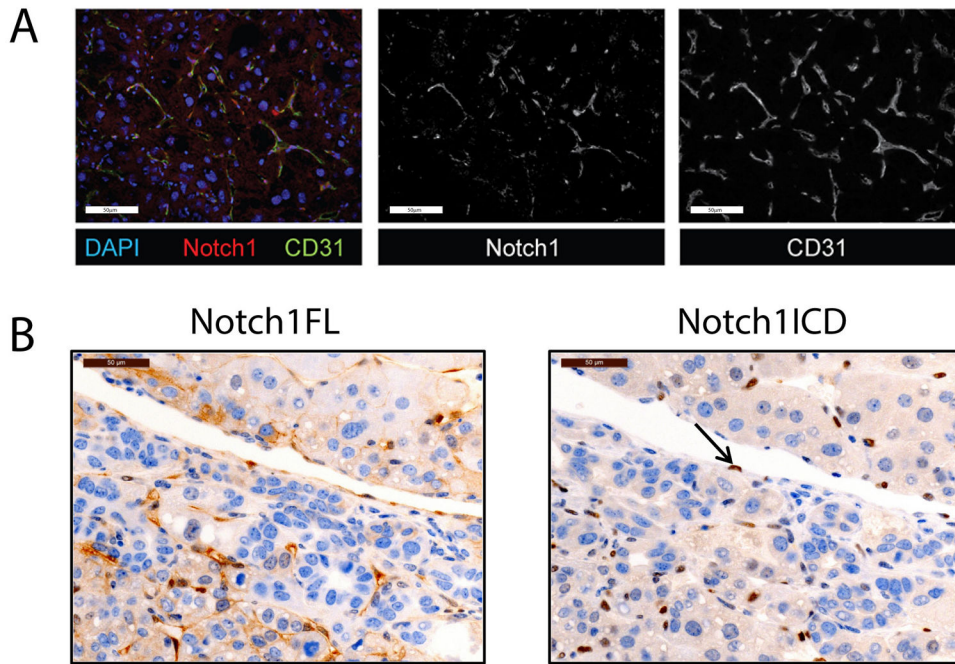
Figure 2.
Notch1 is expressed and active primarily in non-tumor cells. (A) AKT/Ras HTV livers (5 weeks) were stained for Notch1 and CD31 by immunofluorescence. Notch1 was expressed primarily in CD31 positive endothelial cells. (Scale Bar = 50μm) (B) Notch1 was also detected by immunohistochemistry in AKT/Ras livers. In some instances, tumor epithelium stained strongly for membranous Notch1 by IHC (left panel). However, these same areas stained negative for the γ-secretase-cleaved, activated form of Notch1, indicating that Notch1 signaling was not active, except in endothelial cells (right panel, arrow). All analyses were performed on livers five weeks following HTV injection. (Scale Bars = 50μm)
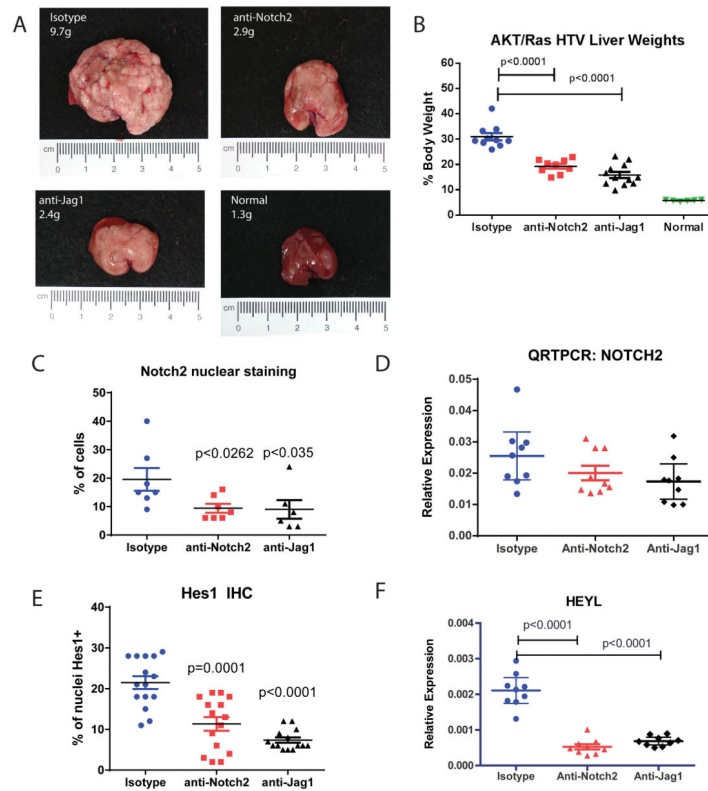
Figure 3.
Inhibition of Notch2 signaling through Notch2 or Jag1 antagonism decreased tumor burden in the AKT/Ras tumor model. (A,B) AKT/Ras HTV mice were injected with anti-Notch2 or anti-Jag1 antibody beginning on the day of the HTV and throughout the five week experiment. Either treatment significantly impeded tumor development (A,B; $p<0.0001$, n>8). (C) Immunofluorescence staining and quantitative morphometry were performed to determine the degree of Notch2 nuclear localization, a measure of Notch2 pathway activation. This analysis revealed both anti-Notch2 and anti-Jag1 treatments diminished Notch2 activation by about half ($p<0.2$, n>5). Values represent nuclear Notch2 positive cells as a fraction of all nucleated cells per liver cross-section. (D) QRTPCR demonstrated there was no decrease in notch2 mRNA expression. (E) Morphometric quantification of Hes1 immunohistochemistry for Notch signaling in AKT/Ras HTV tumor-bearing livers. This Hes1 staining was significantly diminished in animals treated with either the anti-Notch2 or the anti-Jag1 antibody ($p<0.0001$, n>10). (F) Expression of Notch pathway target gene, heyL, was significantly decreased upon treatment with either anti-Notch2 or anti-Jag1 ($p<0.0001$, n>7). All p-values were calculated using Student's t-test.
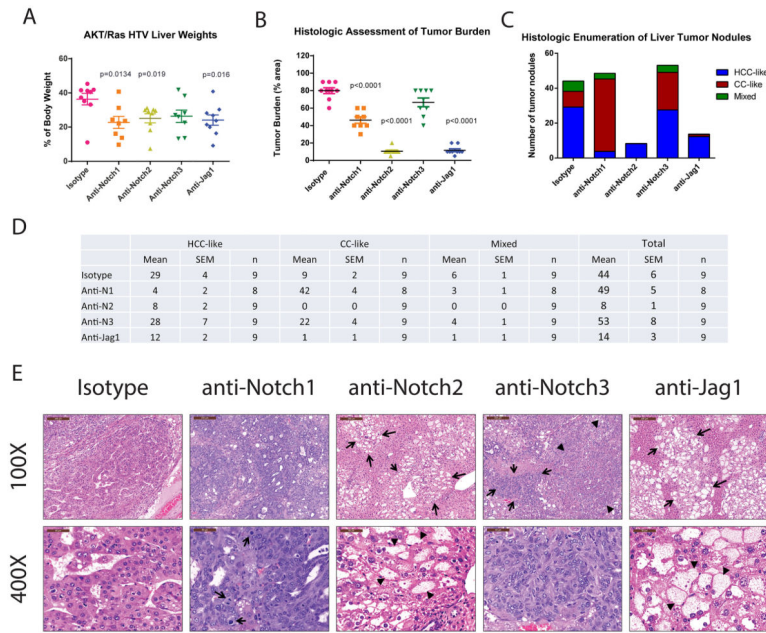
Figure 4.
Effect of Notch pathway modulation on tumor type prevalence in the AKT/Ras HTV model. (A) Liver weight as a % body weight. Livers from isotype control treated AKT/Ras HTV mice enlarged to almost 40% of body weight. Treatment with either anti-Notch2 or anti-Jag1 led to a significant decrease in liver weight (p<0.02; n=9). Inhibition of Notch1 signaling also led to decreased liver weight (p<0.02, n=8), while Notch3 inhibition had no significant effect. Antibody treatment began on the day of HTV injection and continued through the five week experiment. All p-values were calculated using Student's t-test. B) Histological evaluation of liver tumor burden. (C&D) Quantification of morphologic types of liver tumors by histologic evaluation of H&E stained sections. With anti-Notch2 and anti-Jag1 treatment, tumor burden decreased across all tumor types. Anti-Notch1 treatment decreased HCC-like tumors and increased CC-like tumors. Anti-Notch3 treatment did not have a notable effect on tumor number or relative abundance. (E) AKT/Ras mice liver histology of H&E stained sections. Tumors were HCC-like, arranged in broad trabeculae, or were CC-like, with a ductular/pseudoglandular pattern. The CC-like foci predominated in the anti-Notch1 treated livers and had features of aggressive malignancy including frequent mitotic figures (second panel set, arrows) and cellular atypia. Histologic evaluation of liver from anti-Notch2 or anti-Jag1 treated AKT/Ras mice showed predominantly altered hepatocyte foci (top middle and last panel, arrows). 400x magnification (middle and last panels, arrowheads). Anti-Notch3 treated hepatic tumors were similar to isotype control-treated mice with both HCC-like morphology (fourth panel, arrowheads) and CC-like morphology (fourth panel, arrows). (Magnification 100X (top row) or 400X (bottom row), scale bars = 50μm)
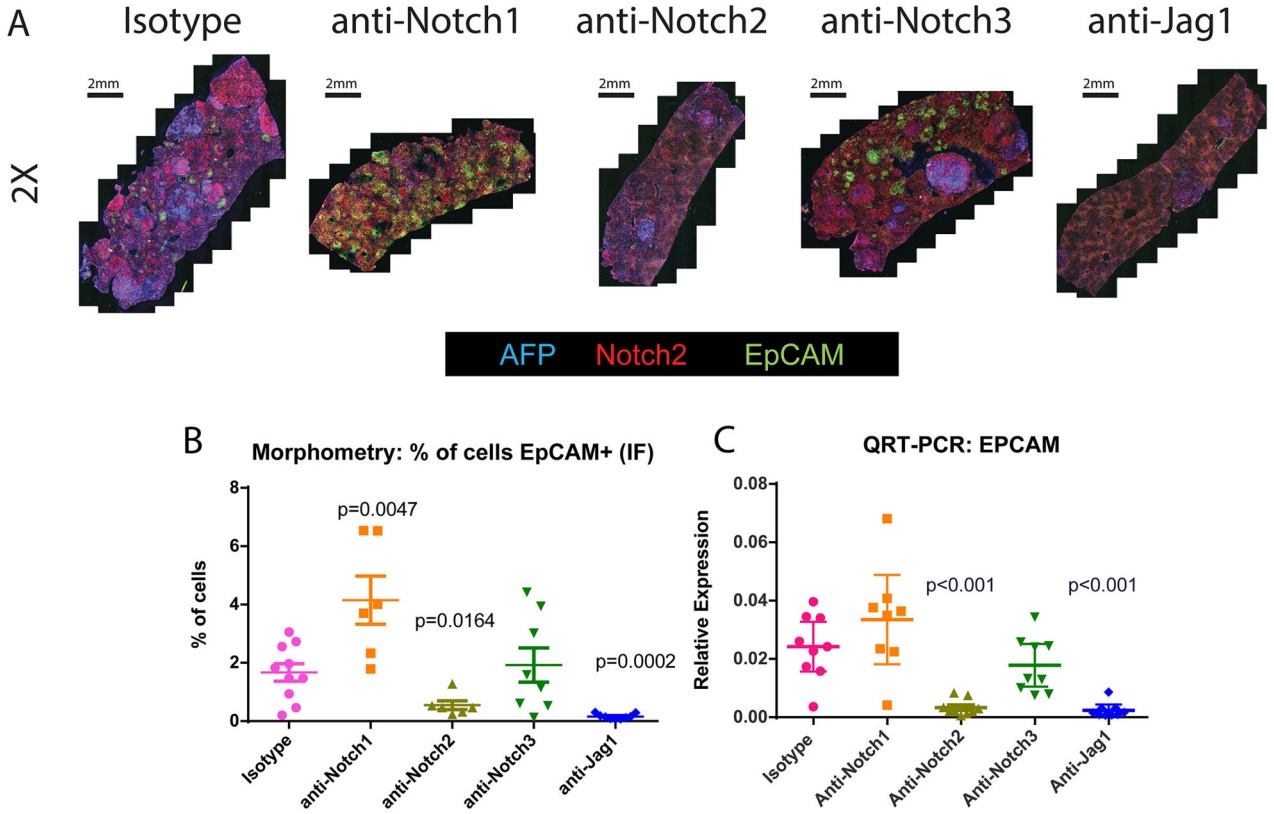
Figure 5.
Effect of antibody treatment on tumor marker expression. (A) Immunofluorescence detection of the HCC marker, AFP, and the CC marker, EpCAM. Isotype control treated livers showed a mixture of AFP-positive and EpCAM-positive tumor nodules, while anti-Notch3 livers looked very similar, with no change in the expression pattern of these tumor markers. In contrast, anti-Notch2 and anti-Jag1-treated livers showed very few, if any, EpCAM positive tumors and a few, isolated AFP positive tumors. Anti-Notch1 treated livers showed few AFP positive tumors but increased EpCAM positive tumors. (Magnification 2X) (B) Quantitative morphometry of marker prevalence in immunofluorescence stained liver sections showed a significant decrease in EpCAM with both anti-Notch2 (p<0.02, n=8) and anti-Jag1 treatment (p<0.0001, n=9). Anti-Notch1 inhibitory antibody increased the extent of EpCAM positive tumors (D; p<0.02, n=7). Notch3 inhibition had no effect. Values represent EpCAM positive cells as a percent of all nucleated cells per whole liver section. (C) Examination of EpCAM transcript by QRT-PCR. Both anti-Notch2 and anti-Jag1 treatment resulted in significant decrease in EpCAM expression (p<0.001, N 8). Neither anti-Notch1 nor anti-Notch3 treatment had a significant effect on EpCAM transcript. All p-values were calculated using Student's t-test.
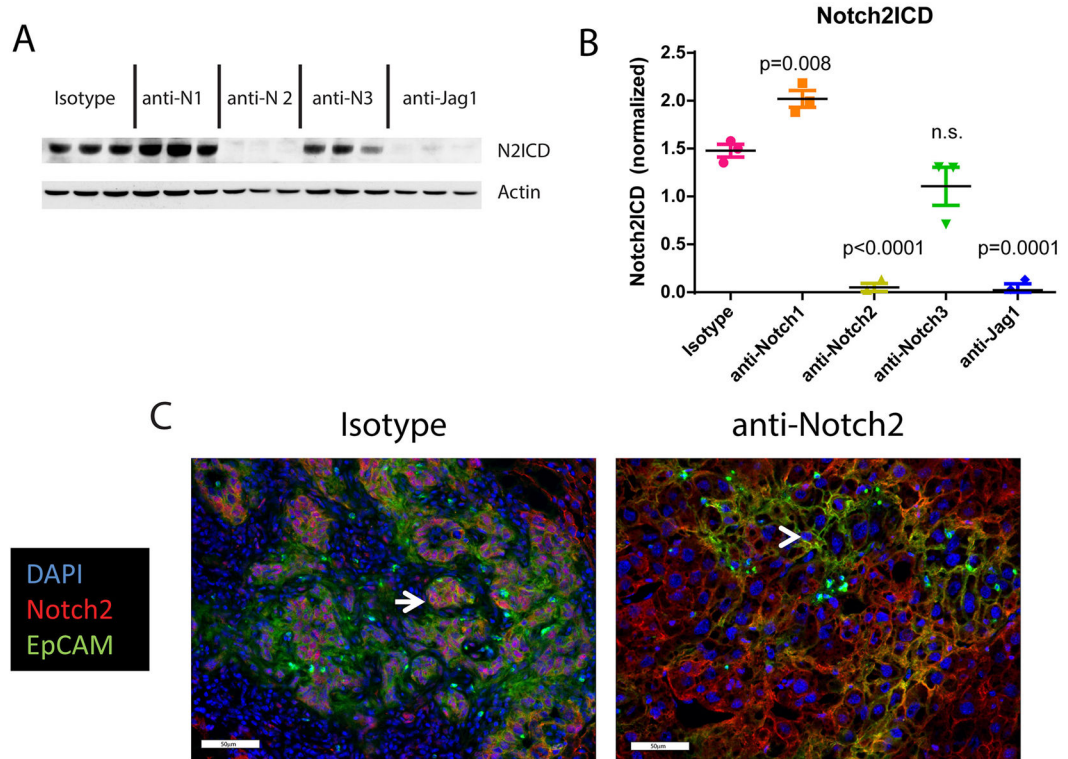
Figure 6.
Notch2 activation was modulated by antibody treatments. (A) Western blotting for the active form of Notch2 (N2ICD) showed that both anti-Notch2 and anti-Jag1 treatment decreased Notch2 activation. (B) Quantification of N2ICD by western blot showed a significant increase (p=0.008;n=3) in average band intensity with anti-Notch1 treatment and a significant decrease with both anti-Notch2 (p<0.0001;n=3) and anti-Jag1 treatment (p=0.0001;n=3). Band intensities were normalized to actin loading control. (C) High power images of a representative EpCAM positive tumor from an isotype-treated AKT/Ras mouse with distinct nuclear Notch2 staining (left panel). Anti-Notch2 treated liver showed lack of nuclear Notch2 staining in an EpCAM positive tumor (Magnification 400X, scale bars = 50µm). All p-values were calculated using Student's t-test.
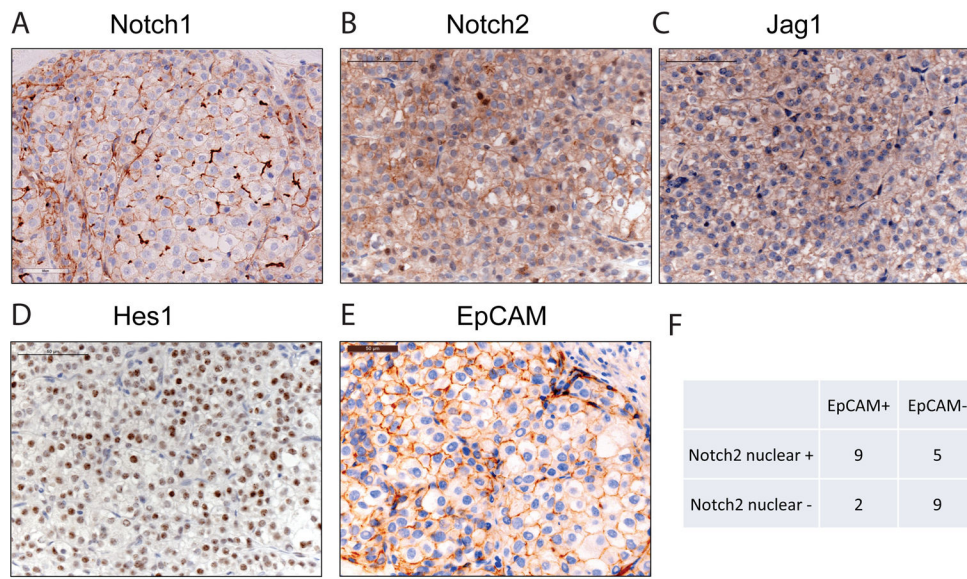
Figure 7. Notch pathway and EpCAM expression in human HCC
Human HCCs were examined for expression of Notch pathway proteins and EpCAM by immunohistochemistry. A selected human hepatocellular carcinoma case is shown which expresses (A) Notch1, (B) Notch2, (C) Jag1, (D) Hes1, and (E) EpCAM in the neoplastic hepatocytes. While there is membranous staining of tumor cells with both Notch1 and Notch2, only Notch2 shows nuclear localization, indicating activation of that receptor. Notch pathway activation is further evidenced by strong Hes1 staining. (F) There is a frequent association between EpCAM positivity and activation of Notch2. Accordingly, we found that the majority of nuclear Notch2 positive cases (64%) were EpCAM positive, while the majority of nuclear Notch2 negative cases (82%) were EpCAM negative. All images 400X magnification. Scale bars = 50 μm.